Extended Abstracts of the 2003 International Conference on Solid State Devices and Materials, Tokyo, 2003, pp. 44-45

B-2-4

Two-Mode Behavior in Time and Temperature Dependence of Imprint-Induced Charge Loss in Integrated $SrBi_2(Ta,Nb)_2O_9$ Capacitors

Atsushi Noma, Takumi Mikawa, Yoshihisa Nagano, Yuji Judai, and Eiji Fujii
ULSI Process Technology Development Center, Semiconductor Company, Matsushita Electric Industrial Co., Ltd.
19, Nishikujo-Kasuga-cho, Minani-ku, Kyoto 601-8413, Japan
Phone: +81-75-662-8911 Fax: +81-75-662-6196 e-mail: noma.atsushi@jp.panasonic.com

1. Introduction

Imprint is one of the most critical reliability issues of ferroelectric capacitors, because it leads to the readout failure of FeRAMs by the loss of retained charge written oppositely with a preliminary poled direction [1]. In order to deduce the imprint mechanism, analytical studies on time and temperature dependence of the imprint-induced charge loss are required. Although several authors have reported the stretched exponential [2] or the logarithmic [3] time-dependent behavior, the background physical mechanism is not fully understood. In this paper, we describe a new concept of the imprint mechanism based on two-mode behavior of the imprint-induced charge loss observed in integrated $SrBi_2(Ta,Nb)_2O_9$ (SBTN) capacitors.

2. Experimental

The samples used for this study are SBTN stacked capacitor arrays integrated on 0.18µm CMOS logic wafers fabricated using the 4-level metal and p-SiN passivation process. The size of an each capacitor is $1.3\mu m^2$ and the thickness of SBTN is 100nm. The details of the capacitor structure are described elsewhere [4].

Fig. 1(a) shows the pulse sequences used for our measurement. At first, a pair of complementarily poled capacitors was baked at different temperatures for a selective period of time. During this baking process, the preliminary poled state was imprinted. Then, the poled state was switched to the opposite direction, and subsequently, the switching and non-switching readout charge of the opposite state (Q_{ossw} and Q_{osns}) was measured at room temperature. The retained charge at the opposite state (Q_{os}) was defined as the half value of the charge difference $Q_{ossw} - Q_{osns}$ as shown in Fig. 1(b). We obtained the time-dependent change of Q_{os}, which represents the imprint-induced charge loss, by repeating these sequences until the cumulative baking time up to 1000h.

3. Results and Discussion

Time Dependence

Fig. 2 shows the time-dependent change of Q_{os} for different baking temperatures, where the vertical axis is normalized against the initial value Q_0. The decay behavior at 85 or 110ºC has only non-linear dependence on a log scale over the whole time range. However, at the temperatures of 125, 150, and 175ºC the linear logarithmic region follows the non-linear region. The change from non-linear to logarithmic takes place when Q_{os}/Q_0 arrives at a particular threshold value (C_{th}) independent of temperature. Since the increase in the baking temperature merely accelerates the decay behavior, the behavior at 85 or 110ºC should also have the logarithmic dependence in the longer baking time.

The decay behavior is re-plotted according to the stretched exponential form [2] in Fig. 3, where a linear relationship can be identified for the time range corresponding to the non-linear region in Fig. 2. This indicates that the decay behavior in this region follows the stretched exponential function.

Therefore, these results reveal that the time-dependent behavior of Q_{os} has two regions: the stretched exponential and the following logarithmic region. This two-mode behavior can be formulated by the following expressions:

$$Q_{os}/Q_0 = \exp[-(R_1 t)^n] \qquad Q_{os}/Q_0 \geqq C_{th}\,, \qquad (1)$$
$$Q_{os}/Q_0 = C_{th} - R_2 \ln(t/t_{th}) \qquad Q_{os}/Q_0 \leqq C_{th}\,, \qquad (2)$$

where R_1 is the decay rate in the stretched exponential region, t is the baking time, n is the stretching factor, R_2 is the decay rate in the logarithmic region, and t_{th} is the time when Q_{os}/Q_0 arrives at C_{th}.

Temperature Dependence

The decay rate R_1 and R_2 in the above equations can be determined from the slope and the intercept of the fitted thick solid lines drawn in Fig. 2 or Fig. 3 for each baking temperature. Fig. 4 shows Arrhenius plots of the temperature dependence of R_1 and R_2. The temperature dependence of R_1 almost obeys the Arrhenius relation, but it tends to saturate slightly with increasing temperature. More strangely, R_2 decreases as temperature increases. The key to understanding of these results is "Curie-Weiss effect" explained in the following.

We confirmed that the retained charge at the imprinted state (Q_{is}) has classical Curie-Weiss dependence on the baking temperature as shown in Fig. 5. Since the rate of thermal imprint is approximately proportional to Q_{is}, which is a driving force of imprint [5], the decrease in Q_{is} at elevated temperature reduces the decay rate R_1 or R_2 as follows:

$$R_x = r_x Q_{is} = r_x [A(T_c - T)]^{1/2} \quad (x = 1 \text{ or } 2)\,, \qquad (3)$$

where r_x is the decay rate per unit Q_{is}, A is a constant, T_c is the Curie temperature, and T is the baking temperature. Therefore, the anomalous results mentioned above are attributed to the reduction of decay rate due to the decrease in Q_{is} at elevated temperature. We called this effect "Curie-Weiss effect" in this paper.

To exclude the Curie-Weiss effect from the measured R_1 and R_2, we calculated r_1 and r_2 in eq. (3), which are plotted in Fig. 6. The temperature dependence of r_1 gave a better fit to the Arrhenius relation, where the activation energy was estimated to be 0.89eV. On the contrary, it was found that r_2 has no temperature dependence. Accordingly, the intrinsic temperature dependence can be specified by the following equations:

$$r_1 = C_1 \exp(-E_a / kT)\,, \qquad (4)$$
$$r_2 = C_2\,, \qquad (5)$$

where E_a is the activation energy, k is the Boltzmann constant, and C_1 and C_2 are constants.

Imprint Mechanism

The origin of thermal imprint is the charge motion for stabilizing the polarized domains in ferroelectric thin films. In the previous reports, it has been proposed that either charged oxygen vacancies [6] or electrons [7] relate to this charge motion. However, we are sure that both of them must be involved at the same time, because our finding of the two-mode behavior, i.e. the two regions with different temperature dependence, is a strong evidence for the simultaneous existence of the two distinct processes as follows.

The activation energy of 0.89eV obtained in the stretched exponential region agrees well with the reported value of 0.91eV for oxygen vacancies to migrate in the perovskite lattice [8]. Thus, it is reasonable to consider that this region corresponds to the reorientation process of the charged oxygen vacancies within the oxygen octahedron as illustrated in Fig. 7(a). On the other hand, the logarithmic-time-dependent behavior with no temperature dependence is quite similar to the discharge behavior of MNOS devices, which is explained by the electron migration by the tunneling process through the nitride and oxide thin film [9]. This analogy supports the view that the logarithmic region corresponds to the electron migration by the tunneling process through the ferroelectric thin film as illustrated in Fig. 7(b).

4. Conclusions

It has been observed that the time-dependent behavior of the imprint-induced charge loss in integrated SBTN capacitors is divided to the stretched exponential region and the following logarithmic region for the first time. By excluding the Curie-Weiss effect, the activation energy in the stretched exponential region is estimated to be 0.89eV. On the contrary, the logarithmic region has no temperature dependence. From this two-mode behavior, we propose a new concept of the imprint mechanism that both of the reorientation process of oxygen vacancies and the electron migration by tunneling process are simultaneously involved.

References

[1] M. Grossmann et al., *Appl. Phys. Lett.*, **76**, 363 (2000).
[2] J. Kim et al., *Integrated Ferroelectrics*, **33**, 133 (2001).
[3] Y. Shimada et al., *Appl. Phys. Lett.*, **71**, 2538 (1997).
[4] Y. Nagano et al., to be published in 2003 VLSI Symposium.
[5] W. L. Warren et al., *Appl. Phys. Lett.*, **68**, 1681 (1996).
[6] G.Arlt et al., *Ferroelectrics*, **87**, 109 (1988).
[7] W. L. Warren et al., *Jpn. J. Appl. Phys.*, **35**, 1521 (1996).
[8] W. L. Warren et al., *J. Am. Ceram. Soc.*, **79**, 536 (1996).
[9] L. Lundkvist et al., *Solid-State Electronics*, **16**, 811 (1973).

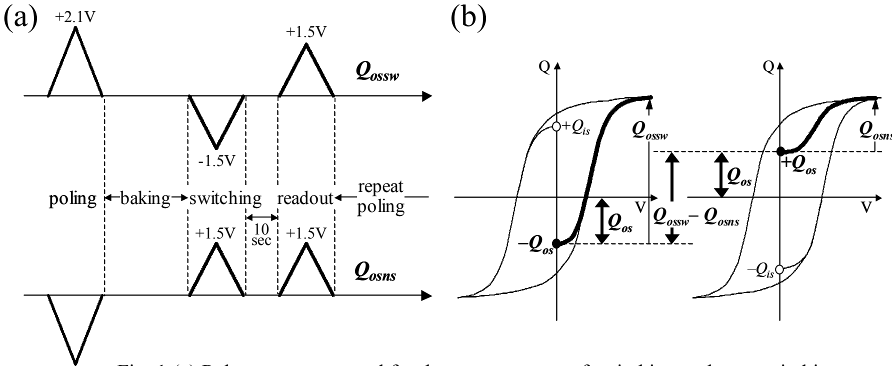

Fig. 1 (a) Pulse sequences used for the measurement of switching and non-switching readout charge (Q_{ossw} and Q_{osns}). (b) Definition of the retained charge at the opposite state (Q_{os}) illustrated in the hysteresis curves of complementarily polarized capacitors.

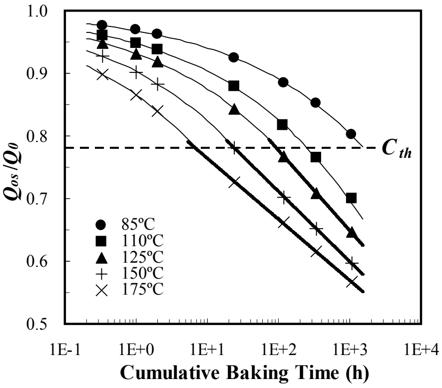

Fig. 2 Time-dependent change of Q_{os} for different baking temperatures.

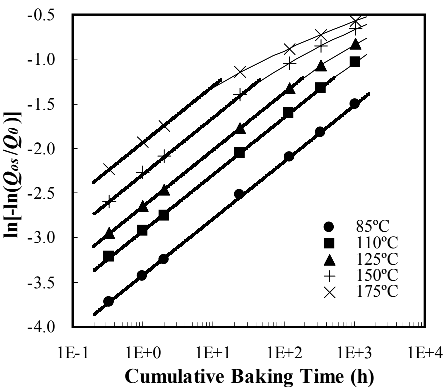

Fig. 3 Stretched exponential plots of the decay behavior of Q_{os} for different baking temperatures.

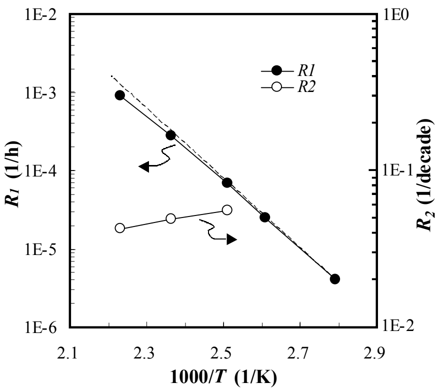

Fig. 4 Arrhenius plots of temperature dependence of the decay rate R_1 and R_2.

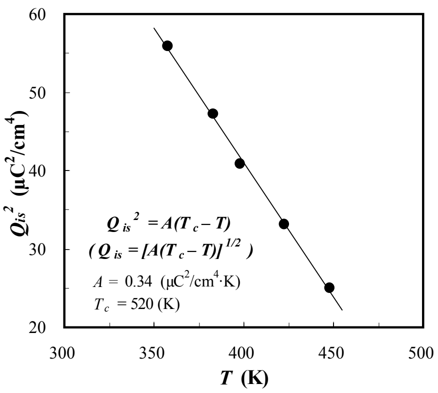

Fig. 5 Retained charge at the imprinted state (Q_{is}) as a fuction of baking temperature.

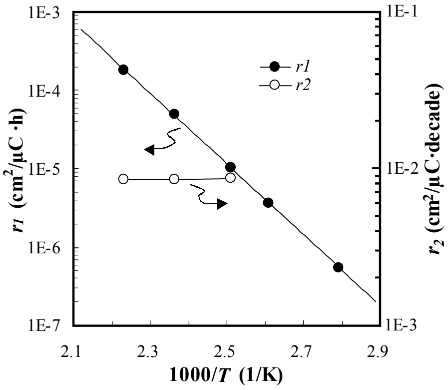

Fig. 6 Arrhenius plots of temperature dependence of the decay rate r_1 and r_2.

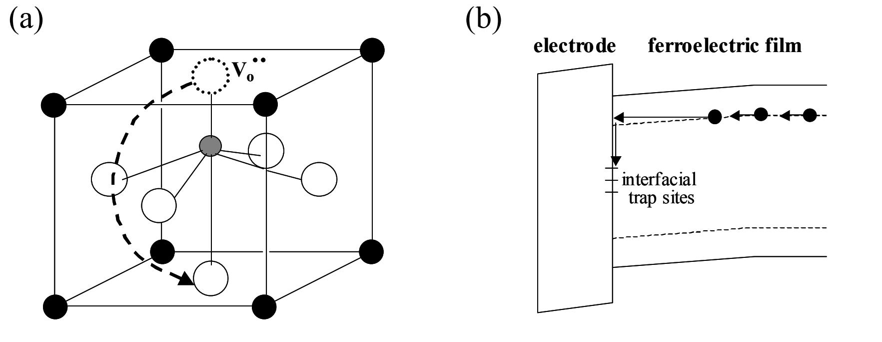

Fig. 7 Schematic diagram of (a) the reorientation process of an oxygen vacancy ($V_o^{\cdot\cdot}$) within an oxygen octahedron of a perovskite lattice and (b) the electron migration by tunneling process through a ferroelectric thin film into the interfacial trap sites.